JOURNAL of the MEXICAN CHEMICAL SOCIETY

https://www.jmcs.org.mx/

Article

Open Access

J. Mex. Chem. Soc. **2026**, *70(1):e2410*

Received December 15th, 2024
Accepted November 28th, 2025

http://dx.doi.org/10.29356/jmcs.v70i1.2410
e-location ID: 2410

Keywords:
Silver nanoparticles; nanomaterials; design of experiments; cytotoxicity; cell viability

Palabras clave:
Nanopartículas de plata; nanomateriales; diseño de experimento; citotoxicidad; viabilidad celular

***Corresponding author:**
Carmen Gonzalez
email: gonzalez.castillocarmen@uaslp.mx
Phone: +52 444-826-2300, ext. 6459

ISSN-e 2594-0317

Size-Specific Synthesis and Biological Evaluation of Silver Nanoparticles: A Computational and Experimental Integration

Aída J. Velarde-Salcedo[1], Karen O. Ruiz-Reyes[1], Gabriela Navarro-Tovar[1,2], Carmen Gonzalez[1*]

[1]Facultad de Ciencias Químicas, Universidad Autónoma de San Luis Potosí. Manuel Nava 6, Zona Universitaria, 78210, San Luis Potosí, S.L.P., México.
[2]Secretaría de Ciencia, Humanidades, Tecnología e Innovación, Insurgentes Sur 1582, Credito Constructor, Benito Juarez, 03940, Mexico City, México.

Abstract. During the last years, nanomaterials, such as silver nanoparticles (AgNPs), have revolutionized various areas due to their antimicrobial properties. However, their impact on human health in the short, medium, and long term has yet to be fully understood due to the variability in their sizes and the lack of standards that define a specific size and their biological impact. Specialized software can help develop mathematical models and predict the conditions necessary to produce AgNPs of a controlled size. These tools complement experimental techniques, facilitating physical-chemical characterization and contributing to a more precise regulation and safe use of AgNPs in various applications. This study aimed to determine the optimal conditions for the chemical synthesis of AgNPs of different sizes through the design of experiments (DOE) to optimize the synthesis conditions and to evaluate their effects in the NIH-3T3 cell line. A 2^4 DOE was carried out, varying the temperature, reaction time, concentration of the precursor agent, and concentration of the reducing agent, using the nanoparticle size as a response variable supported by the MiePlot software. AgNPs were characterized by ultraviolet-visible light absorption spectroscopy, dynamic light scattering, and transmission electron microscopy. It was possible to synthesize and characterize the AgNPs with a predominant size of 60 nm, which conditions were also complemented with the MiePlot

J. Mex. Chem. Soc. **2026**, *70(1):e2410*
Regular Issue

ISSN-e 2594-0317

software. It was found that temperature and the concentration of reducing agents influence nanoparticle size and that the smaller the nanoparticle, the more significant toxicity they exhibit in NIH-3T3 cells. The present study shows the value of the complementary use of computational tools like MiePlot integrated with experimental methods for the size-specific synthesis of AgNPs. These findings provide a reference point for comparing and predicting the biological effects of similarly sized AgNPs, offering a broader framework for their safe and controlled application in various fields.

Resumen. Durante los últimos años, los nanomateriales, como las nanopartículas de plata (AgNPs), han revolucionado diversas áreas debido a sus propiedades antimicrobianas. Sin embargo, su impacto en la salud humana a corto, mediano y largo plazo aún no se comprende completamente debido a la variabilidad en sus tamaños y la falta de estándares que definan un tamaño específico y su impacto biológico. El software especializado puede ayudar a desarrollar modelos matemáticos y predecir las condiciones necesarias para producir AgNPs de un tamaño controlado. Estas herramientas complementan las técnicas experimentales, facilitando la caracterización físico-química y contribuyendo a una regulación más precisa y al uso seguro de las AgNPs en diversas aplicaciones. Este estudio tuvo como objetivo determinar las condiciones óptimas para la síntesis química de AgNPs de diferentes tamaños mediante el diseño de experimentos (DOE) para optimizar las condiciones de síntesis y evaluar sus efectos en la línea celular NIH-3T3. Se llevó a cabo un DOE 2^4, variando la temperatura, el tiempo de reacción, la concentración del agente precursor y la concentración del agente reductor, utilizando el tamaño de la nanopartícula como variable de respuesta apoyada por el software MiePlot. Las AgNPs se caracterizaron mediante espectroscopía de absorción de luz ultravioleta-visible, dispersión de luz dinámica y microscopía electrónica de transmisión. Fue posible sintetizar y caracterizar las AgNPs con un tamaño predominante de aproximadamente 60 nm, cuyas condiciones también se complementaron con el software MiePlot. Se encontró que la temperatura y la concentración de agentes reductores influyen en el tamaño de las nanopartículas y que cuanto más pequeña es la nanopartícula, mayor toxicidad exhiben en las células NIH-3T3. El presente estudio muestra el valor del uso complementario de herramientas computacionales como MiePlot integradas con métodos experimentales para la síntesis específica de AgNPs por tamaño. Estos hallazgos proporcionan un punto de referencia para comparar y predecir los efectos biológicos de AgNPs de tamaño similar, ofreciendo un marco más amplio para su aplicación segura y controlada en diversos campos.

Abbreviations

AgNPs, silver nanoparticles
ANOVA, analysis of variance
ATCC, American Type Culture Collection
BHMIE, Bohren-Huffman-Mie algorithm
DLS, Dynamic Light Scattering
DMEM, Dulbecco's Modified Eagle Medium
DOE, Design of Experiments; h.d., hydrodynamic diameter
LDH, Lactate dehydrogenase
LSPR, Localized Surface Plasmon Resonance
MTT, 3-[4,5-dimethylthiazol-2-yl]-2,5-diphenyltetrazolium bromide
OECD, Organization for Economic Cooperation and Development
PBS, Phosphate buffered saline solution
PVA, Polyvinyl acetate
R^2, coefficient of determination
R^2_{adj}, adjusted coefficient of determination
R^2 PRESS, Predicted Residual Sum of Squares coefficient of determination
TEM, Transmission Electron Microscopy
UV-Vis, ultraviolet visible

Introduction

Silver nanoparticles (AgNPs) are currently found in commercial products such as medical devices, food packages, feminine hygiene products, textiles, among others, due to their strong antimicrobial activity [1]. When AgNPs are synthetized by chemical reduction, the Ag^+ ions from a metal precursor (e.g. silver nitrate, silver chloride) are reduced to Ag^0 through the action of a reducing agent (sodium citrate, hydrazine, fructose),

http://dx.doi.org/10.29356/jmcs.v70i1.2410

J. Mex. Chem. Soc. **2026**, *70(1):e2410*
Regular Issue

ISSN-e 2594-0317

and a stabilizing agent (polyethylene glycol, chitosan, sodium citrate) prevents the aggregation of nanoparticles to obtain a defined shape [2–6]. Chemical reduction allows to obtain a wide variety of sizes from 7 nm to 500 nm, and different morphologies such as nanocubes, nanowires and nanospheres, depending on the reaction conditions (temperature, pH, time of reaction, the nature and concentration of the reagents used, etc.) [4]. This variability shows that there is still much to understand in how the synthesis conditions affect the final product and its stability, and it is necessary to standardize/optimize AgNPs production process by this method to obtain a homogeneous product with true applicability in the industry.

Despite the advantages and applications that AgNPs offer, the exposure to manufacturing AgNPs-containing products is associated with potential health problems. In this sense, their toxicity depends on the particle size, shape, surface charge, composition, and stability [7]. A general observation is that the smaller the nanoparticle, the greater the toxicity it will present, as cellular uptake is facilitated by smaller nanoparticles [8]. Small nanoparticles can easily traverse the mesh-like organization of the extracellular matrix (20- 40 nm), pass the cell membrane through clathrin-coated pits (100-350 nm) or caveolae- mediated process (20-100 nm), and even enter the cell nucleus by passive diffusion through pores (6-9 nm) or importin-supported active transport (up to 50 nm) [9]. Despite that AgNPs have been used for decades, the toxicity and their mechanisms of action in function of: 1) morphology, 2) concentration, 3) capping and functionalization, 4) exposure time, 5) route of exposure, 6) interaction with biological components and their microenvironment, 7) bioaccumulation and biodistribution, as well as the impact in humans health in the short, medium and long term has not yet been fully explored. Rohde et al. (2021) reported that AgNPs (25 nm with polymer cover, 2.5 to 5 µg/mL) may induce lipid peroxidation leading in proteotoxicity and necrosis, while Ag^{+1} (0.3 to 2.7 µg/mL) released from the nanoparticles increases oxidative stress with later apoptotic cell death in SUM159 breast cancer cells and immortalized mammary epithelial cells [10]. Moreover, AgNPs can induce DNA damage, activate phosphorylation of proteins, alter the mitochondrial membrane potential, increase the levels of inflammatory cytokines (e.g. IL-8, TNF-α), induce cell-cycle arrest in the G/M phases, among other alterations, which are reported as both concentration and size-dependent [11]. Furthermore, adverse effects linked to Ag^{+} released from AgNPs include permanent bluish-gray discoloration of the skin or eyes, liver damage, kidney damage, eye irritation, respiratory tract problems, intestinal disorders, and adverse changes in blood cells [12]. Because AgNPs are commonly present in paints, coatings and roofing, they can be eliminated with rainwater and directed to the soil; when functionalized fabrics are washed AgNPs are filtered into wastewater and subsequently spread on agricultural fields [13]. Therefore, it is crucial to study in detail the conditions in which AgNPs can be synthetized with determined morphology and size to prevent toxic effects in humans and the environment.

In this respect, the design of experiments (DOE) is a poorly applied tool in the synthesis of nanoparticles, and it may optimize time and the chemical conditions, to maximize their benefits, minimize their costs and risks, contributing to their effective and safe use with the obtention of tuned nanoparticles. DOE is the planning and carrying out of a set of tests to obtain data which will later be analyzed statistically and will allow obtaining information about certain situations for decision making [14]. DOE's objective is to obtain as much information as possible about the case study and the importance lies in the validation of the project, and at the same time it allows a level of control for process or product improvements. DOEs are used in multiple areas and industries such as chemistry, mechanics, materials science, industrial engineering, and electronics. The most common applications include control of chemical synthesis reactions, crystallization processes, polymerization reactions, control of bioprocesses, among others [15,16].

The aim of this study was to develop a 2^4 fractional factorial experimental design to determine the optimal conditions for the AgNPs synthesis, according to the nanoparticles size. A mathematical model was obtained based on the data generated and the model was validated experimentally. Synthetized AgNPs were later characterized, and their potential toxicity was tested in the NIH-3T3 mouse fibroblast cell line.

Materials and methods

Design of experiments

To determine how the AgNPs size changes with respect to certain experimental conditions, an optimized 2^4 fractional factorial experimental design was carried out using the JMP® Pro-16.2.0 statistical software (JMP Statistical Discovery LLC, Cary, NC, USA). The factors evaluated were temperature (X_1),

http://dx.doi.org/10.29356/jmcs.v70i1.2410

J. Mex. Chem. Soc. **2026**, *70(1):e2410*
Regular Issue

ISSN-e 2594-0317

synthesis reaction time (X_2), concentration of the precursor agent $AgNO_3$ (X_3) and concentration of sodium citrate (as the reducing/stabilizer agent, X_4). Each factor was evaluated at two different levels and with a central point as shown in Table 1. The fixed variables were the volume (20 mL of $AgNO_3$ and 2.5 mL of sodium citrate) and the pH of the solutions (pH 7.0). A total 20 syntheses in 2 blocks (experiments per day) were performed by duplicate. The estimated nanoparticle size was established as the response variable, which was determined by Ultraviolet-Visible (UV-Vis) spectroscopy and applying Mie theory with the Mieplot v46.21 program [17] that is a simulation software for nanoparticle spectra according to their localized surface plasmon resonance (LSPR) (UV-Vis signal between 400 and 500 nm) and allows to predict particle sizes from 12 nm up to 20 nm [18].

Table 1. Factors and levels used for the design of experiments.

Factors	Low level	High level	Central point
Temperature (X_1)	60 °C	90 °C	75 °C
Reaction time (X_2)	10 min	30 min	20 min
Concentration of $AgNO_3$ (X_3)	0.5 mM	1 mM	0.75 mM
Concentration of sodium citrate (X_4)	17 mM	51 mM	34 mM

Synthesis of AgNPs

Synthesis of AgNPs was performed following the Frens method with $AgNO_3$ and sodium citrate [19]. Reactions were covered from light and prior to synthesis, all the material was treated with a 15 % HCl, 5 % HNO_3 solution and washed three times with deionized water to eliminate any residue. Then, 20 mL of $AgNO_3$ (Merck KGaA, Darmstadt, Germany) solution was placed with constant stirring and controlled temperature in a hotplate stirrer (LabTech, Mexico City, Mexico), 2.5 mL of sodium citrate solution (Avantor, Allentown, PA, USA) were added, and time was clocked according to DOE. Successful synthesis was visually determined if a color shifting was present in the solution. All experiments were at room temperature for 30 min and samples were centrifuged at 600 x g for 30 min in a Sorvall Biofuge Primo R (Thermo Fisher Scientific Inc., Waltham, Massachusetts, USA). Supernatant was discarded, AgNPs were resuspended in 2 mL of deionized water, and stored at 4 °C under dark conditions.

UV-Vis spectroscopy and particle size estimation

AgNPs were sonicated in a BenchMark Pulse 150 tip ultrasonic homogenizer (BenchMark Scientific, Sayreville, NJ, USA) for 5 minutes at 2-second intervals with a 40% power and a 2 mm tip to promote homogenization of the suspension. A quartz cell with 2 mL of deionized water was used as blank, subsequently 2 mL of the homogenized AgNPs suspension was added to the quartz cells and read in a TM7350 UV-Visible single beam spectrophotometer (Cole-Parmer, Vernon Hills, IL, USA) in a range of 200 to 800 nm. From the spectra and LSPR obtained by UV-Vis, a comparison with the MiePlot software was made; if the wavelength where the highest absorbance peak is found and both spectra were equal, it was assumed that they have the same estimated nanoparticle size.

Hydrodynamic diameter

AgNPs hydrodynamic diameter (h.d.) in nm was determined in a Delsa™ Nano C Particle Analyzer (Beckman Coulter Life Sciences, Brea, CA, USA) (He-Ne laser at room temperature; h.d.: wavelength 633 nm, detection angle at 90°, lapse 60s). Measurements were conducted only on syntheses that exhibited high-quality UV-Vis spectra, characterized by well defined and symmetric LSPR peaks with minimal baseline noise. Samples were measured by triplicate.

Transmission Electron Microscopy (TEM)

AgNPs colloid selected to analyze morphology using TEM were treated as follow: AgNPs were diluted in ethanol, three drops were taken and deposited dropwise onto a formvar-carbon grid 300 mesh EMR®, the

J. Mex. Chem. Soc. **2026**, *70(1):e2410*
Regular Issue

ISSN-e 2594-0317

organic solvent was evaporated at room temperature, and the sample was then analyzed in a JEOL 1010 60Kv Microscope (Jeoul Ltd., Peabody, MA, USA).

Cell culture

To evaluate the potential damage or toxicity that AgNPs of different sizes could exert, the mouse fibroblast NIH-3T3 cell line was used (American Type Culture Collection, ATCC, Manassas, VA, USA). Cells were cultured in Dulbecco's Modified Eagle Medium (DMEM, Thermo Fisher Scientific Inc.) supplemented with 10 % fetal bovine serum (Thermo Fisher Scientific Inc.), 1 % streptomycin/penicillin solution (Thermo Fisher Scientific Inc.) in a 5 % CO_2 atmosphere at 37 °C in a HERACell Bios 16i incubator (Thermo Fisher Scientific Inc.). $1.5x10^3$ cells/well were seeded in 96-well plates and allowed to reach confluence. Cells were then washed with phosphate buffered saline solution (PBS, 2.63 mM KCl, 1.46 mM KH_2PO_4, 136.89 mM NaCl, 13.5 mM $Na_2HPO_4 \cdot 7H_2O$, pH 7.4), complete culture medium was added along with 84 µg/mL of AgNPs of different sizes and incubated for 48 h. 0.5 % of Triton X100 (Merck KGaA) was used as a positive control of cell damage.

Lactate dehydrogenase (LDH) cytotoxicity assay

After treatments, 100 µL of media were collected and transferred to a new plate to evaluate the LDH activity using the Cytotoxicity Detection Kit (Merck KGaA). A 25 µL volume of reaction mix were added to the media samples, incubated at 37°C for 45 min and absorbances were read at a 492 nm wavelength in an iMark microplate reader (Bio-Rad Laboratories Inc., Hercules, CA, USA). The formation of formazan red is directly correlated with the LDH released to the medium after cell damage. Cytotoxicity was calculated with the equation:

$$Citotoxicity\ (\%) = \frac{(Abs_{Treated\ cells} - Abs_{Non-treated\ cells})}{(Abs_{Cells\ treated\ with\ Triton\ X100} - Abs_{Non-treated\ cells})}$$

Cell viability

Cell viability (mitochondrial activity) of treated cells was determined with the MTT Cell Proliferation Kit I (Merck KGaA). After treatments 10 µL of MTT solution 1 (5 mg/mL 3-[4,5-dimethylthiazol-2-yl]-2,5-diphenyltetrazolium bromide in PBS) were added to the cells with 100 µL of culture media and the plates were incubated at 37 °C for 4 h. Blue formazan crystals were then solubilized with 100 µL of MTT solution 2 (10 % SDS in 10 mM HCl) and incubated at 37 °C overnight. Absorbance of the simples was measured a 562 nm in an iMark microplate reader (Bio-Rad Laboratories Inc.). Cell viability was calculated and expressed as a percentage by comparing treatments with untreated cells.

Validation of the experimental design and statistical analysis

At the end of the syntheses of the experimental design, the JMP statistical software was used, where the different approximate sizes of the nanoparticles (obtained from LSPR signal and UV-Vis spectrum in MiePlot) were entered to obtain the factors and interactions that had a significant effect on the synthesis of the AgNPs using the analysis of variance (ANOVA) with a significance level of $p<0.05$. Then, an equation was obtained to describe the formation of the AgNPs. The coefficient of determination (R^2) and the adjusted coefficient of determination (R^2_{adj}) were obtained, and two new experimental syntheses were carried out to verify the predictive capacity of the statistical model.

Similarly, one-way ANOVA and Tukey's test with a significance level of $p<0.05$ were performed using JMP on the results of the toxicological evaluation of the different sizes of AgNPs, each test was done in triplicate and the average was plotted with the standard deviation using the GraphPad Prism Software v9.3.0 (GraphPad Software Inc., La Jolla, CA, USA).

Results

DOE and AgNPs synthesis

From DOE a total of 20 experiments were carried out with different combinations of the factors following the established parameters. One of the physical and qualitative indicators of the formation of AgNPs

J. Mex. Chem. Soc. **2026**, *70(1):e2410*
Regular Issue

ISSN-e 2594-0317

was the change in color of the solution from colorless to yellow. Only 14 conditions were appropriate for the formation of AgNPs. Certain levels of factors did not favor the synthesis of AgNPs, such as the 4 factors at their lowest level (60°C, 10 min of reaction time, 0.5 mM $AgNO_3$ and 17 mM sodium citrate). Moreover, the conditions that must be present for a successful synthesis of AgNPs were high levels of all factors (Supplementary Table S1).It is worth noting that the DOE matrix included repeated experimental conditions to estimate pure error and evaluate reproducibility, such as experiments 2 and 18 (60 °C, 30 min, 1 mM $AgNO_3$, 51 mM sodium citrate), experiments 7 and 14 (60 °C, 30 min, 1 mM $AgNO_3$, 51 mM sodium citrate) and experiments 13 and 20 (90 °C, 30 min, 1 mM $AgNO_3$, 17 mM sodium citrate). In these runs variations in the particle size obtained were observed, despite identical synthesis parameters, i.e. experiments 2 and 18 yielded estimated sizes of 50 and 45 nm, respectively, whereas experiments 13 and 20 both yielded 50 nm.

Characterization of AgNPs

The presence of AgNPs was confirmed by UV-Vis spectrophotometry in the range of 200 – 800 nm. The specific LSPR spectra of the AgNPs revealed an absorption peak in the range of approximately 404 – 482 nm, reaffirming the presence of AgNPs in all 14 solutions. A representative spectrum of a successful AgNPs synthesis (experiment 17) is shown in Fig. 1, and a summary of all experimental are found in Supplementary Table S1. In this example, the wavelength of the highest absorption peak was observed at 413 nm; if the spectrum is compared with the theoretical data from MiePlot program corresponding to spherical 55 nm AgNPs, it is observed that both have the largest absorption peak at the same wavelength (Fig. 1**(A)**). Therefore, it was estimated that the conditions of experiment 17 lead to the synthesis of nanoparticles of 50 nm in size. This comparison was done for all 14 successful experiments and the approximate sizes obtained were 45, 50, 55, 60, 70, 75 and 100 nm, being 60 nm the most predominant size.

To confirm the approximate size results estimated by MiePlot software, five syntheses of AgNPs (experiments 5, 8, 13, 17 and 19) were characterized with dynamic light scattering (DLS). The selection of these experiments was based on the results of the absorption spectra obtained by UV-Vis, that is, those which exhibited a noise-free spectrum and a more pronounced absorption peak. The syntheses selected for characterization were representative of the range of nanoparticle sizes obtained in the DOE. Although not all successful syntheses were analyzed by DLS, the subset chosen provides reliable data for comparison with MiePlot estimations. For experiment 17, the hydrodynamic ratio obtained was 66.4 nm with a polydispersity of 0.315 (Fig. 1**(B)**); which when compared with MiePlot theoretical size, represents a 17.16 % difference. For experiments 5, 8, 13 and 19, the differences were 9.50 %, 4.89 %, 12.89 % and 19.23 %, respectively.

Three successful syntheses were selected from DLS for analysis by TEM, considering the samples with the lowest polydispersity values and that represented different nanoparticle sizes, which corresponded to experiments 5, 13 and 17. With these syntheses, a comparative analysis was carried out, using the results of MiePlot and TEM. Fig. 1**(C)** shows the micrography of AgNPs from experiment 17, which led to the formation of oval-shaped nanoparticles with a size close to 57.09 nm. When the size was compared to the size predicted by MiePlot (55nm), it represented a 3.66 % difference (Supplementary Table S1). From the percentage of error (differences in particle sizes) of MiePlot calculated with DLS and TEM, it was observed that TEM had a lower difference than DLS.

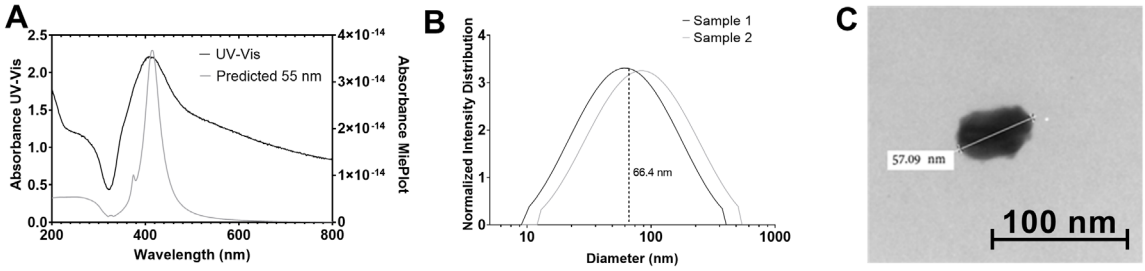

Fig. 1. Characterization of a successful AgNPs synthesis (experiment 17). **(A)** Comparison of UV-Vis spectrum (black dotted line) with a predicted 55 nm spectrum from MiePlot Software (gray dotted line). **(B)** Dynamic Light Scattering superposed particle distribution, suggesting a hydrodynamic ratio of 66.4 nm. **(C)** Micrography of AgNP showing a particle size around 57.09 nm, obtained by Transmission Electron Microscopy.

http://dx.doi.org/10.29356/jmcs.v70i1.2410

J. Mex. Chem. Soc. **2026**, *70(1):e2410*
Regular Issue

ISSN-e 2594-0317

Statistical analysis and DOE validation

To identify how the variables and conditions tested influenced the nanoparticle size, once the experiments were completed, results obtained by MiePlot were analyzed and an ANOVA test was performed. Statistical analysis and model parameters are shown in Table 2. F values identified whether the model contained factors that represented a statistically significant effect on the synthesis of AgNPs (Pr F<0.0001) using the least squares criterion, with a 95 % significance level, which indicated that the synthesis of AgNPs was significantly affected by one or several factors.

Then, factors and interactions were evaluated with Student's t test to determine significance. Those factors that did present a significant difference were temperature (X_1) and concentration of sodium citrate (X_4) and the interactions that significantly affected were temperature with reaction time (X_1X_2), temperature with $AgNO_3$ concentration (X_1X_3), reaction time with concentration of sodium citrate (X_2X_4), concentration of $AgNO_3$ with concentration of sodium citrate (X_3X_4), temperature with concentration of $AgNO_3$ and with concentration of sodium citrate ($X_1X_3X_4$), reaction time with concentration of $AgNO_3$ and with concentration of sodium citrate ($X_2X_3X_4$) and finally the interaction of the four factors temperature, reaction time, concentration of $AgNO_3$ and concentration of sodium citrate ($X_1X_2X_3X_4$, Table 2).

To determine the quality of the model, R^2 was interpreted, with a value obtained of 0.9702, indicating that 97% of the response variability could be explained by the model. R^2_{adj}, which indicates the significance of the model, and the percentage of variability in the response, eliminating those variables that are not transcendental for the real variable, was 0.9372 or 93.72%. The Predicted Residual Sum of Squares coefficient of determination (R^2 PRESS), which evaluates the predictive capacity of the statistical model was 0.87, indicating that there is 87% predictive capacity for next data that can be entered [14].

The coefficients of the significant factors and interactions were obtained through multiple regression analysis and the first-order polynomial equation that defines the predicted response was obtained (Y) in terms of the independent variables (X_1, X_2, X_3 and X_4).

$$Y = 43.22 + 7.50X_1 + 8.84X_4 + 6.25X_1X_2 + 8.04X_1X_3 - 11.00X_1X_4 + 11.34X_2X_4 - 6.88X_3X_4 + 15.96X_1X_3X_4 + 5.63X_2X_3X_4 - 11.54X_1X_2X_3X_4$$

Where, Y is the predicted response, i.e. the AgNPs size, X_1 is the encoded value of the temperature, X_4 is the encoded value of the sodium citrate concentration. The negative values of the interaction coefficients shown in the equation mean that a high level of both factors can cause a decrease in the nanoparticle size, and in the same way when there is a positive value in the interaction coefficient it means that at low levels an increase in the nanoparticle size is obtained.

Table 2. Statistical analysis of DOE.

Analysis of variance						**Factors and interactions with a significant difference in the model**		
	DF	**Sum of squares**	**Square average**	**F ratio**	**Prob>F**	**Variables**	**Prob> |t|**	**Model coefficient**
Model	10	17138.898	1713.89	29.3893	<0.0001	Constant	<0.0001	43.22
Error	9	524.582	58.32			Temperature (X_1)	0.0025	7.50
C. Total	19	17663.750				Sodium citrate concentration (X_4)	0.0008	8.84
Model quality parameters						X_1X_2	0.0073	6.25
		R^2	0.9702			X_1X_3	0.0016	8.04
		R^2_{adj}	0.9372			X_1X_4	0.0002	-11.00
		R^2 PRESS	0.87			X_2X_4	0.0001	11.34

J. Mex. Chem. Soc. **2026**, *70(1):e2410*
Regular Issue

ISSN-e 2594-0317

	R^2	0.9702		X_3X_4	0.0043	-6.88
				$X_1X_3X_4$	<0.0001	15.96
				$X_2X_3X_4$	0.0126	5.63
				$X_1X_2X_3X_4$	0.0001	-11.54

In different contour plots is observed that to reduce the nanoparticle size, the concentration of sodium citrate must be decreased and in the same way the reaction temperature must be decreased (Fig. 2**(A)**). On the other hand, increasing the reaction time and increasing the temperature will result in a larger nanoparticle size (Fig. 2**(B)**). If the nanoparticle size is required to be decreased, the temperature can be increased whereas the $AgNO_3$ concentration is decreased (Fig. 2**(C)**). Moreover, increasing the concentration of $AgNO_3$ and the reaction time, the nanoparticle size increases (Fig. 2**(D)**). Fig. 2**(E)** represents an affinity towards a nanoparticle size from 40 nm to 50 nm. Finally, Fig. 2**(F)** shows that to increase the nanoparticle size it could also be necessary to increase the amount of sodium citrate and decrease the amount of $AgNO_3$.

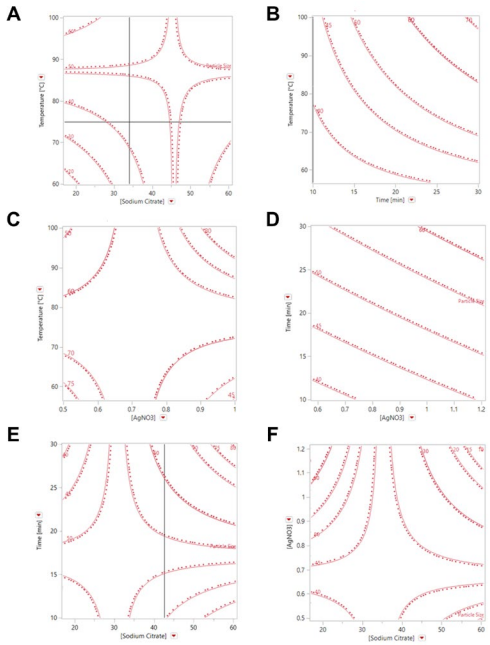

Fig. 2. Contour plots of the statistical model that show the interactions between factors upon AgNPs size. **(A)** Concentration of sodium citrate (17-51 mM) and temperature (60-90 °C) **(B)** Temperature and reaction time (10-30 min) **(C)** Temperature and concentration of $AgNO_3$ (0.5-1.0 mM) (D) Reaction time and concentration of $AgNO_3$ **(E)** Reaction time and concentration of sodium citrate **(F)** Concentration of sodium citrate and concentration of $AgNO_3$.

To validate the model equation, two syntheses were performed using the prediction profiler of JMP software, with different conditions that were not previously tested in the DOE. The first synthesis was carried out at a temperature of 90 °C, 51 mM sodium citrate, 15 min reaction time and 1 mM $AgNO_3$, with a predicted nanoparticle size of 59.83 nm. The suspension obtained was analyzed by UV-Vis and the absorption spectrum was compared with MiePlot, confirming a nanoparticle size of 60 nm, which represents a 0.28 % difference with the predicted size. (Fig. 3**(A)**). For the second synthesis, the conditions were adjusted to a temperature of 90 °C, 17 mM sodium citrate, 20 min of reaction and 0.5 mM of $AgNO_3$, with a predicted size of 53 nm. UV-Vis spectrum suggested a nanoparticle size of 50 nm for this experiment, representing a 5.6 % difference with the predicted size (Fig. 3**(B)**).

http://dx.doi.org/10.29356/jmcs.v70i1.2410

J. Mex. Chem. Soc. **2026**, *70(1):e2410*
Regular Issue

ISSN-e 2594-0317

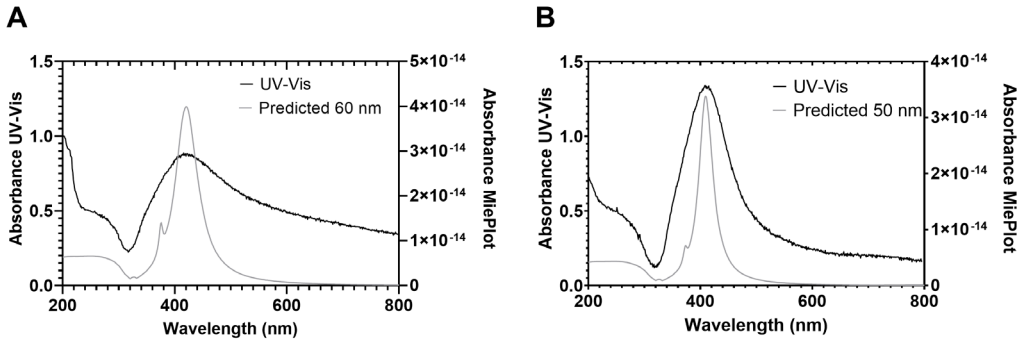

Fig. 3. Experimental validation of the mathematical model obtained with the DOE. **(A)** Synthesis was carried out at 90 °C, 51 mM of sodium citrate, 1 mM of $AgNO_3$ for 15 min and 60 nm AgNPs were expected. **(B)** Synthesis was carried out at 90 °C, 17 mM of sodium citrate, 0.5 mM of $AgNO_3$ for 20 min and 53 nm AgNPs were expected. Absorption spectra (black dotted line) were compared to MiePlot software (gray dotted line) to estimate the nanoparticle size.

Toxicological evaluation of AgNPs in mouse fibroblasts

NIH-3T3 cells were treated with AgNPs of different sizes for 48 h (50, 55, 60, 70 and 75 nm) and then tested for cytotoxicity and cell viability using the LDH and MTT assays, respectively. The control group (untreated cells) indicates the lowest possible cytotoxic effect; the treatment with Triton X100 detergent was used as a control of cell lysis and considered as 100 % of cytotoxicity [20]. When cells were treated with AgNPs, an increase in cytotoxicity was observed as the nanoparticle size decreased, and the values of larger sizes presented significant differences along with the size of 50 nm with respect to the control (Fig. 4**(A)**). The 50 nm AgNPs presented a larger cytotoxicity than the one observed with Triton X100. On the other hand, the cell viability response obtained with untreated cells was considered as a 100 % of viability (Fig. 4**(B)**), and Triton X100 significantly reduced the viability, to the point no formazan blue was formed, suggesting there were no viable cells. In a similar way to the cytotoxicity test, treatment with AgNPs showed that 55 and 50 nm decreased cell viability, whereas nanoparticles of 60 and 70 nm showed a viability similar than untreated cells, and 75 nm nanoparticles increased viability up to 15 %. Sizes of 50, 60, 70 and 75 nm were statistically different to the control.

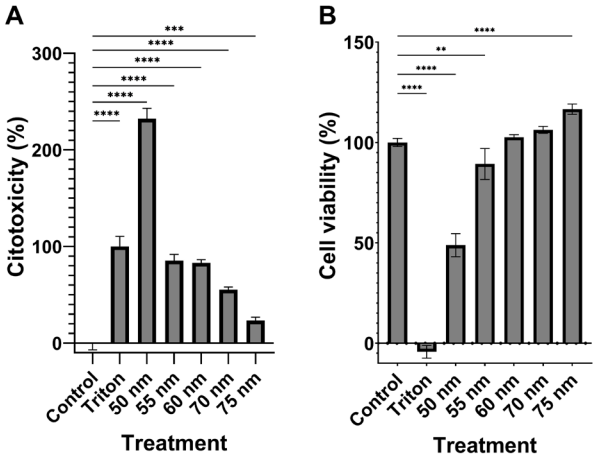

Fig. 4. Effect of AgNPs of different sizes upon the viability of NIH-3T3 cells. Mouse fibroblast cells were treated with 84 µg/mL of AgNPs for 48 h. **(A)** Cells were tested for LDH cytotoxicity assay, results are expressed as a percentage or response (mean ± SD) when compared to cells treated with Triton X100. **(B)** Cells were tested for cell viability; results are expressed as percentage of response (mean ± SD) when compared to untreated cells. Triton X100 was used as a control of cell damage. **p<0.01, ***p<0.001, ****p<0.0001.

http://dx.doi.org/10.29356/jmcs.v70i1.2410

J. Mex. Chem. Soc. **2026**, *70(1):e2410*
Regular Issue

ISSN-e 2594-0317

Discussion

AgNPs can be synthesized with different methods, and nanoparticles of different sizes can be obtained; therefore, DOE could be a useful tool to establish the experimental conditions to obtain a particular nanoparticle size, and to a better understanding of how the variables can influence the result of the synthesis. With the experimental approach of this study, it was observed that only 14 out of the 20 experiments performed allowed the successful synthesis of AgNPs. The factors related to the nanoparticle size were temperature and sodium citrate concentration; and all the interaction levels of these factors also influenced the nanoparticle size, which ranged from 45 to 100 nm, being 60 nm the most predominant size. Other studies that used Frens-based methodology have reported similar results for AgNPs synthesis. Dong et al. (2009) used citrate and $AgNO_3$ in a stepwise reaction varying pH and found that initial pHs of 6.9 and 7.7 (closed to pH 7.0 used in our study) improved shape control to spherical nanoparticles compared with the typical one-step reaction, and obtained particles around 71 and 58 nm, respectively [21]. Islam et al. (2021) agree that using $AgNO_3$ and sodium citrate during the synthesis results in spherical nanoparticles with a size range of 24 to 132 nm [2]. Khodashenas & Ghorbani (2009) reported that when using sodium citrate as a stabilizing agent, the AgNPs acquire a size of 30 to 60 nm, with a spherical shape [22]. Finally, Yerragopu et al. (2020) obtained sizes from 34 nm to 85 nm [23]. All these reports have in common that quasi-spherical nanoparticles are obtained, and the most frequent size ranges are between 50 and 70 nm, which is in accordance with our results. Smaller citrate-capped AgNPs can also be obtained, however, to achieve this, a more potent reducing agent must be used. Quintero-Quiroz et al. (2019) used DOE to optimize the synthesis of AgNPs using sodium borohydride as reducing agent and sodium citrate as stabilizing agent, varying the concentration of $AgNO_3$ (10-90 mM), sodium citrate (10-90 mM), sodium borohydride (10-90 mM) and pH (8-12). They synthesized AgNPs of different sizes (12-37 900 nm) and found that the concentration of sodium citrate has a greater effect on the size of the nanoparticles, whereas sodium borohydride influences polydispersity [24].

For the characterization of the AgNPs synthetized UV-Vis, DLS and TEM techniques were used. UV-Vis showed the characteristic LSPR spectra of AgNPs that allowed to estimate the nanoparticle size with MiePlot. Mie theory can be used to calculate the extinction cross section of a particle and describe its theoretical color (based on the propagation of electric and magnetic fields and their interaction with different objects). Mie theory provides an alternative to calculate absorption and extinction coefficients allowing the estimation of nanoparticles to be approximated by the position of surface plasmons, material of the nanoparticles and the dielectric permittivity of the medium [25]. MiePlot is a free and open access software that uses the Bohren-Huffman-Mie (BHMIE) algorithm for the analytical resolution of Maxwell's equations and leads to obtaining the optical behavior of the LSPR [17,26], this facilitates the optimization of chemical and time resources during initial screening. However, it also has limitations, including a resolution of ±5 nm, the assumption of ideal spherical geometry without accounting for the solvation layer, and the inability to provide morphological or polydispersity information. For these reasons, MiePlot should be considered a complementary rather than a replacement tool for direct characterization techniques. This approach, however, could be extended beyond AgNPs to other metallic or dielectric particles (e.g. AuNPs, CuNPs) that exhibit well-defined LSPR [18].

DLS was used to determine the hydrodynamic radius of AgNPs of five experiments, resulting in five different sizes and polydispersion rates. Polydispersity indicates the heterogeneity of the nanoparticle in a solution [27]. The result must be within the range of 0 to 1, with 0 being a monodisperse solution and 1 being a solution with greater size variability, and the smaller the polydispersity value, the reading is more reliable [28]. Only one result was below 0.3 and the others were below of 0.4, this indicates that the solutions had some size variability. Furthermore, hydrodynamic radius refers to the nanoparticle size plus the electric dipolar layer of the surface caused by the movement of the AgNPs in the liquid, therefore variation is expected. When the hydrodynamic radiuses were compared with the values obtained by MiePlot, it was observed that the experiments with the lower polydispersity showed a greater accordance with the estimated value.

For the characterization with TEM, three syntheses were analyzed, and the differences between MiePlot estimated sizes and TEM (considered as the real size) were lower than 7 %. This was expected because, for TEM analysis, the samples are in a dried state, instead of fluctuating in a liquid. Therefore, it can be concluded that MiePlot is a viable and sustainable alternative to preliminarily estimate the nanoparticle sizes when characterization techniques are not available, because it requires only UV-Vis spectra and free downloadable software. This approach can optimize the use of resources such as time and chemical reagents; however, its resolution is limited to the size estimation in 5 nm increments.

J. Mex. Chem. Soc. **2026**, *70(1):e2410*
Regular Issue

ISSN-e 2594-0317

Moreover, a first order equation was obtained from the analysis of DOE with all the factors studied and their interactions, which was used as a predictive tool for nanoparticle size, as a way of validation of the model. Two different syntheses were performed and the error percentages between the model and MiePlot were lower than 6%, reaffirming the validity of the model and confirming the value of the determination coefficients, which remained above 85%. The observed size variations between replicated experiments performed under identical conditions are consistent with the inherent sensitivity of chemical nanoparticle synthesis to minor uncontrolled variations. Factors such as small temperature fluctuations (±1-2 °C) [21], trace impurities in reagents, or subtle differences in addition rate, stirring intensity, or timing can create microgradients in concentration or temperature during nucleation, ultimately influencing particle growth [4,21]. Similar effects have been reported for citrate-mediated AgNP synthesis, where variations in mixing and reagent addition significantly impacted particle size and morphology [21]. In our case, the inclusion of replicated runs enabled us to consider this variability in the model and confirm it did not significantly compromise its statistical robustness or predictive capability. Determination coefficients determine how much variability of the response values can be explained by the experimental factors and their interactions. The value must be between 0 and 1, and the closer it is to 1, the stronger or more accurate the model will be and the better it will predict the response [29]. To our knowledge there are only two studies where DOE was carried out for the synthesis of AgNPs. Cuervo-Osorio et al. (2020) used temperature, $AgNO_3$ concentration, polyvinyl acetate (PVA) and sodium citrate as factors, of which only PVA did not affect the nanoparticle size [30]. The difference in why some authors find factors that significantly affect them, and others do not, not only depends on the factor itself, but also on the levels being worked on. In our study, the factors that individually affect the nanoparticle size were temperature and sodium citrate. Cuervo-Osorio et al. used two temperature levels (80 °C and 100 °C) being somewhat like the levels of this work; however, the authors used 0.1 M and 0.2 M concentrations of $AgNO_3$, this factor being significant in their model, and very different from the concentrations proposed in this report. Li et al. (2012) used DOE with three factors with three levels each. The main parameters that affected the nanoparticle size were the concentration of the reducing agent (sodium hypophosphite) and the temperature (30, 40 and 50 °C) [7], according with our results.

Regarding the biological evaluation of AgNPs of different sizes it was found that the smaller the nanoparticle size, the greater the toxic effects occur in NIH-3T3 cells. This effect may be due to the absorption and release of metal ions. The interaction mechanisms that are involved between AgNPs and living systems are not yet fully detailed, but it is known to be related to the capacity of the AgNPs to penetrate and modify the cells homeostasis, being the smaller nanoparticles the ones that enter more easily and react with oxygen to produce toxic silver ions and reactive oxygen species, ending in biomolecules damage (e.g. DNA) [31]. The NIH-3T3 cell line of murine fibroblasts is a biological model widely to evaluate cellular effects (viability or toxicity), viruses' characterization, and deoxyribonucleic acid transfection [32], it has been reported to be sensitive to silver ions [33], and is the cell line recommended by the Organization for Economic Cooperation and Development (OECD) to test the cytotoxicity of manufactured nanomaterials [34]. In this work, AgNPs exhibiting the greatest cytotoxicity were those of 50 nm, followed by 60 nm and 55 nm. This effect was also observed in the viability assay, where a lower percentage of viability was observed in the smaller sizes. Citrate-coated AgNPs of lower sizes have presented toxic effects in different cell lines; Amooaghaie et al., (2015) observed that AgNPs (30 nm) reduced viability of mouse bone marrow derived mesenchymal stem cells [35] Barbasz et al. (2017) observed that AgNPs (14 nm) reduces the viability of human monocytes (U-937) and promyeloblasts (HL-60) cell lines, up to 60 % at 15 mg/L, which was related to cell damage, nitric oxide production and lipid peroxidation ([36]; and the study of Quintero-Quiroz mentioned above reported that AgNPs (12 nm) can be toxic to Vero and NIH-3T3 cells (90 µg/mL) [24]. Furthermore, Bélteky et al (2021) made a comparison of citrate-coated AgNPs of different sizes on the viability of healthy and cancerous human cell lines; AgNPs of 10, 20 and 50 nm showed an IC_{50} of 8.28 ppm, 10.41 ppm and 12.53 ppm on the DU145 human prostate cancer cell line, respectively, and an IC_{50} of 1.96 ppm, 3.08 ppm and 11.67 ppm on HaCaT immortalized human keratinocyte cells, respectively [37], confirming that smaller nanoparticles have greater toxicity as in the smallest AgNPs a lower concentration is needed to reduce cell viability. It is worth to mention that what all these reports have in common, and is different in our study, is they used sodium borohydride as reducing agent in the synthesis to achieve smaller sizes. This reagent is recognized as toxic and in contact with water releases flammable gases, which increases risks during production of AgNPs, along with the demonstrated cytotoxicity of synthesized AgNPs.

http://dx.doi.org/10.29356/jmcs.v70i1.2410

J. Mex. Chem. Soc. **2026**, *70(1):e2410*
Regular Issue

ISSN-e 2594-0317

Conclusions

The results displayed in this study confirm the hypothesis that depending on the nanoparticle size, different effects can be obtained, particularly in the NIH-3T3 mouse fibroblast cell line. A DOE was carried out to obtain AgNPs of different sizes, using UV-Vis spectra and MiePlot software as way to obtain a statistical model, a procedure that was validated with DLS and TEM. Currently there are only a few studies that have performed a statistical analysis to define the size of the AgNPs to be studied. This approach could benefit many projects where specific sizes of NPs are required with the optimization of time and resources; it is expected that this work lays the foundations to continue with this strategy. This research line is of utmost importance because AgNPs are used in multiple articles due to their variety of applications in products or processes in areas of chemistry, polymer science, electrochemistry, medicine, and other areas, where health and environmental safety must be granted.

Acknowledgements

Funding: This work was supported by the Secretaría de Ciencia, Humanidades, Tecnología e Innovación [grant numbers F003-316826 and CF-2023-I-967].

The authors would like to thank to Dr. Denisse de Loera (Laboratory of Synthesis and Photosynthesis) for facilitating the use of the UV-Vis spectrophotometer. The authors also would like to thank to the Laboratory of Polymers in the Instituto de Física (UASLP) and the Laboratory of Electronic Microscopy in the Molecular Pathology Department in the Instituto Nacional de Cancerología for the assessment on DLS equipment, and the obtention of TEM images, respectively.

References

1. McGillicuddy, E.; Murray, I.; Kavanagh, S.; Morrison, L.; Fogarty, A.; Cormican, M.; Dockery, P.; Prendergast, M.; Rowan, N.; Morris, D. *Sci. Total. Environ.* **2017**, *575*, 231-246. DOI: https://doi.org/10.1016/J.SCITOTENV.2016.10.041
2. Islam, M. A.; Jacob, M. V.; Antunes, E. *J. Environ. Manage.* **2021**, *281*, 111918. DOI: https://doi.org/10.1016/J.JENVMAN.2020.111918
3. Natsuki, J.; Natsuki, T.; Hashimoto, Y. *Int. J. Mater. Sci.* **2015**, *4*, 325–32. DOI: https://doi.org/10.11648/J.IJMSA.20150405.17
4. Syafiuddin, A.; Salmiati; Salim, M. R.; Beng Hong Kueh, A.; Hadibarata, T.; Nur, H. *Chin. J. Chem.* **2017**, *64*, 732–56. DOI: https://doi.org/10.1002/JCCS.201700067
5. Sánchez Moreno, M. Máster Universitario en Ciencia y Tecnología Química. Universidad Nacional de Educación a Distancia, 2017.
6. Lee, S. H.; Jun, B. H. *Int. J. Mol. Sci.* **2019**, *20*, 865. DOI: https://doi.org/10.3390/IJMS20040865
7. Li, X.; Wang, L.; Fan, Y.; Feng, Q.; Cui, F. Z. J. *Nanomater.* **2012**, 54838. DOI: https://doi.org/10.1155/2012/548389
8. Haider, A.; Kang, I. K. *Adv. Mat. Sci. Eng.* **2015**, 1–16. DOI: https://doi.org/10.1155/2015/165257
9. Augustine, R.; Hasan, A.; Primavera, R.; Wilson, R.J.; Thakor, A.S.; Kevadiya, B. D. *Mater. Today Commun.* **2020**, *25*, 101692. DOI: https://doi.org/10.1016/j.mtcomm.2020.101692
10. Rohde, M. M.; Snyder, C.M.; Sloop, J.; Solst, S. R.; Donati, G. L.; Spitz, D. R.; Furdui, C. M.; Singh, R. *Part. Fibre Toxicol.* **2021**, *18*, 37. DOI: https://doi.org/10.1186/s12989-021-00430-1
11. Ferdous, Z.; Nemmar, A. *Int. J. Mol. Sci.* **2020**, *21*, 2375. DOI: https://doi.org/10.3390/ijms21072375
12. Prabhu, S.; Poulose, E. K. *Int. Nano Lett.* **2012**, *2*, 1–10. DOI: https://doi.org/10.1186/2228-5326-2-32
13. Pulit-Prociak, J.; Stokłosa, K.; Banach, M. *Environ. Chem. Lett.* **2015**, *13*, 59–68. DOI: https://doi.org/10.1007/S10311-014-0490-2/TABLES/1

J. Mex. Chem. Soc. **2026**, *70(1):e2410*
Regular Issue

ISSN-e 2594-0317

14. Montgomery, D. C., in: *Design and Analysis of Experiments*. 10th ed., Wiley, Hoboken, **2020**.
15. https://www.mt.com/us/en/home/library/white-papers/automated-reactors/Innovative-Techniques-to-Synthesize-Breakthrough-Molecule.html, accessed in October 2024.
16. Montoya-Marquez, J.; Sánchez-Estudillo, L.; Torres-Hernández, P. *Ciencia y Mar.* **2011**, *15*, 61–70.
17. http://www.philiplaven.com/mieplot.htm, accessed in February 2024.
18. Barbir, D.; Dabic, P.; Mehes, M. *Hem. Ind.* **2019**, *73*, 397–404. DOI: https://doi.org/10.2298/HEMIND190719031B
19. Gakiya-Teruya, M.; Palomino-Marcelo, L.; Rodriguez-Reyes, J. C. F. *Methods Protoc.* **2019**, *2*, 3. DOI: https://doi.org/10.3390/MPS2010003
20. Torres, Y.; López, I.; Balderas, I.; Arredondo, E.; González, P.; Ramírez, M. *Revista de Ciencias Farmacéuticas y Biomedicina*. **2017**, *1*, 19.
21. Dong, X.; Ji, X.; Wu, H., Zhao, L.; Li, J.; Yang, W. J. *Phys. Chem. C.* **2009**, *113*, 6573–6. DOI: https://doi.org/10.1021/jp900775b
22. Khodashenas, B.; Ghorbani, H. R. *Arab. J. Chem.* **2019**, *12*, 1823–38. DOI: https://doi.org/10.1016/J.ARABJC.2014.12.014
23. Yerragopu, P. S.; Hiregoudar, S.; Nidoni, U.; Ramappa, K. T.; Sreenivas, A. G.; Doddagoudar, S. R. *Int. Res. J. Pure Appl. Chem.* **2020**, *21*, 37-50. DOI: https://doi.org/10.9734/IRJPAC/2020/V21I330159
24. Quintero-Quiroz, C.; Acevedo, N.; Zapata-Giraldo, J.; Botero, L. E.; Quintero, J.; Zárate-Triviño, D.; Saldarriega, J.; Pérez, V. Z. *Biomater. Res.* **2019**, *23*. DOI: https://doi.org/10.1186/s40824-019-0173-y
25. Colón Figuerona, M. Ingeniería en Materiales. Benemérita Universidad Autónoma de Puebla, 2015.
26. Bohren, C. F.; Huffman, D. R., in: *Absorption and Scattering of Light by Small Particles*. WILEY-VCH Verlag GmbH & Co. KGaA. Weinheim, **1998**. DOI: https://doi.org/10.1002/9783527618156
27. Danaei, M.; Dehghankhold, M.; Ataei, S.; Hasanzadeh Davarani, F.; Javanmard, R.; Dokhani, A.; Khoeasani, S.; Mozafari, M. R. *Pharmaceutics.* **2018**, *10*, 57. DOI: https://doi.org/10.3390/pharmaceutics10020057
28. Bhattacharjee, S. *J. Control Release.* **2016**, *235*, 337–51. DOI: https://doi.org/10.1016/J.JCONREL.2016.06.017
29. Kaushik, R.; Saran, S.; Isar, J.; Saxena, R. K. *J. Mol. Catal. B Enzym.* **2006**, *40*, 121–6. DOI: https://doi.org/10.1016/J.MOLCATB.2006.02.019
30. Jaramillo, M.; Ossa-Orozco, C. P. *Revista ION.* **2020**, *33*, 17–32. DOI: https://doi.org/10.18273/revion.v33n1-2020002
31. Schluesener, J. K.; Schluesener, H. *J. Arch. Toxicol.* **2013**, *87*, 569–76. DOI: https://doi.org/10.1007/S00204-012-1007-Z/FIGURES/3
32. María, D.; Delgadillo Álvarez, C. *Revista Fesahancccal*. **2021**, *7*, 17–24.
33. Jiravova, J.; Tomankova, K. B.; Harvanova, M.; Malina, L.; Malohlava, J.; Luhova, L.; Panacek, A.; Manisova, B.; Kolarova, H. *Food Chem. Toxicol.* **2016**, *96*, 50–61. DOI: https://doi.org/10.1016/J.FCT.2016.07.015
34. Chueh, P. J.; Liang, R. Y.; Lee, Y. H.; Zeng, Z. M.; Chuang, S. M. J. *Hazard Mater.* **2014**, *264*, 303–12. DOI: https://doi.org/10.1016/j.jhazmat.2013.11.031
35. Amooaghaie, R.; Saeri, M. R.; Azizi, M. *Ecotoxicol. Environ. Saf.* **2015**, *120*, 400–8. DOI: https://doi.org/10.1016/j.ecoenv.2015.06.025
36. Barbasz, A.; Oćwieja, M.; Roman, M. *Colloids Surf. B Biointerfaces.* **2017**, *156*, 397–404. DOI: https://doi.org/10.1016/j.colsurfb.2017.05.027
37. Bélteky, P.; Rónavári, A.; Zakupszky, D.; Boka, E.; Igaz, N.; Szerencsés, B.; Kiricsi, M.; Kónya, Z. *Int. J. Nanomedicine.* **2021**, *16*, 3021–40. DOI: https://doi.org/10.2147/IJN.S304138